

See discussions, stats, and author profiles for this publication at: <https://www.researchgate.net/publication/6324818>

1,2-Mannobioside Mimic: Synthesis, DC-SIGN Interaction by NMR and Docking, and Antiviral Activity

ARTICLE *in* CHEMMEDCHEM · AUGUST 2007

Impact Factor: 2.97 · DOI: 10.1002/cmdc.200700047 · Source: PubMed

CITATIONS

42

READS

60

11 AUTHORS, INCLUDING:



[Lorena Martinez](#)

Hospital Universitario Ramón y Cajal

10 PUBLICATIONS 273 CITATIONS

SEE PROFILE



[Franck Fieschi](#)

University Joseph Fourier - Grenoble 1

64 PUBLICATIONS 2,377 CITATIONS

SEE PROFILE



[Pedro M Nieto](#)

Spanish National Research Council

95 PUBLICATIONS 2,130 CITATIONS

SEE PROFILE



[Javier Rojo](#)

Spanish National Research Council

77 PUBLICATIONS 2,575 CITATIONS

SEE PROFILE

1,2-Mannobioside Mimic: Synthesis, DC-SIGN Interaction by NMR and Docking, and Antiviral Activity

José J. Reina,^[a] Sara Sattin,^[b] Donatella Invernizzi,^[b] Silvia Mari,^[b] Lorena Martínez-Prats,^[d] Georges Tabarani,^[c] Franck Fieschi,^[c] Rafael Delgado,^[d] Pedro M. Nieto,^[a] Javier Rojo,^{*[a]} and Anna Bernardi^{*[b]}

The design and preparation of carbohydrate ligands for DC-SIGN is a topic of high interest because of the role played by this C-type lectin in immunity and infection processes. The low chemical stability of carbohydrates against enzymatic hydrolysis by glycosylases has stimulated the search for new alternatives more stable in vivo. Herein, we present a good alternative for a DC-SIGN ligand based on a mannobioside mimic with a higher enzymatic stability than the corresponding disaccharide. NMR and

docking studies have been performed to study the interaction of this mimic with DC-SIGN in solution demonstrating that this pseudomannobioside is a good ligand for this lectin. In vitro studies using an infection model with Ebola pseudotyped virus demonstrates that this compound presents an antiviral activity even better than the corresponding disaccharide and could be an interesting ligand to prepare multivalent systems with higher affinities for DC-SIGN with potential biomedical applications.

Introduction

DC-SIGN (dendritic cell-specific ICAM-3 grabbing nonintegrin) is a tetrameric C-type lectin presenting four copies of a carbohydrate recognition domain (CRD) at the C terminus.^[1–3] This calcium dependent lectin specifically recognizes highly-glycosylated structures present at the surface of several pathogens such as viruses (HIV, SIV, Hepatitis C, Ebola, Cytomegalovirus, Dengue, SARS), bacteria (*Mycobacterium tuberculosis*, *Klebsiella pneumoniae*, *Helicobacter pylori*), yeasts (*Candida albicans*), and parasites (*Leishmania spp.*, *Schistosoma mansoni*).^[4] The main carbohydrate ligand recognized by DC-SIGN is the high mannose glycan, (Man)₉(GlcNAc)₂ also represented as (Man)₉, a branched oligosaccharide which is presented in multiple copies by several pathogen glycoproteins (gp120, GP1, etc.). DC-SIGN plays a key role in the infection process of some of these pathogens and it is considered as an interesting new target for the design of anti-infective agents.

Carbohydrate multivalent display should be an adequate strategy to interact with this lectin with high affinity. The complexity of high mannose structures makes them unlikely candidates for the preparation of multivalent systems with potential applications in biomedicine. However, high mannose presents in all its arms, terminal disaccharides Man α 1-2Man which are likely to be involved in high mannose recognition processes. For instance, the well characterized neutralizing monoclonal antibody 2G12 that recognizes the highly glycosylated HIV glycoprotein gp120 interacts with this disaccharide.^[5,6] Very recently, it has also been demonstrated that high-density arrays of unbranched Man α 1-2Man-terminated oligosaccharides bind to DC-SIGN almost as efficiently as the entire Man₉.^[7] This sug-

gests an important role of the nonreducing end Man α 1-2Man fragment of Man₉ in DC-SIGN recognition.

We have recently reported that compound **1** shares the three-dimensional structure and conformational behavior of Man α 1-2Man **2** (Figure 1) but is more stable to hydrolysis mediated by jack-bean mannosidase.^[8]

Herein, we describe the synthesis of a pseudo-1,2-mannobioside (Man₁,2-psMan-OCH₂CH₂NH₂ **1a**, Scheme 1) designed to allow conjugation of the mimic to polyvalent or solid supports. The molecule was built by connecting a mannose unit to a conformationally locked diol (psMan, R=H in Figure 1), which acts as a mimic of the reducing end mannose ring and

[a] J. J. Reina, Dr. P. M. Nieto, Dr. J. Rojo
Departamento de Química Bioorgánica, Instituto de Investigaciones Químicas, CSIC, Américo Vespucio 49, 41092 Sevilla (Spain)
Fax: (+34) 954460565
E-mail: javier.rojo@iiq.csic.es

[b] S. Sattin, Dr. D. Invernizzi, Dr. S. Mari, Prof. Dr. A. Bernardi
Dipartimento di Chimica Organica e Industriale e CISI, Università di Milano, via Venezian 21, 20133 Milano (Italy)
Fax: (+39) 0250314072
E-mail: anna.bernardi@unimi.it

[c] G. Tabarani, Dr. F. Fieschi
Institut de Biologie Structurale Jean-Pierre Ebel, CEA/CNRS/Université Joseph Fourier, 41 rue Jules Horowitz, 38027 Grenoble (France)

[d] L. Martínez-Prats, Dr. R. Delgado
Laboratorio de Microbiología Molecular, Hospital Universitario 12 de Octubre, Madrid (Spain)

Supporting information for this article is available on the WWW under <http://www.chemmedchem.org> or from the author.

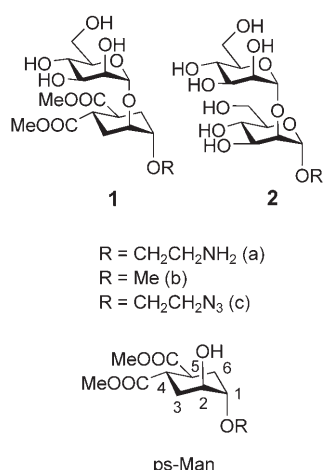
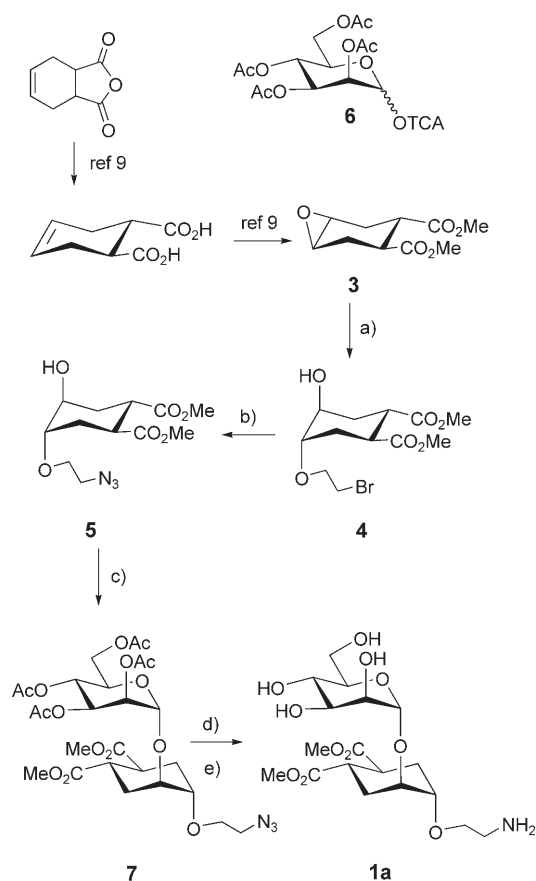


Figure 1. Chemical structure of pseudo-1,2-mannobioside **1**, Man α 1-2Man **2**, and numbering of the ps-Man fragment.



Scheme 1. Synthesis of the pseudomannobioside Man1,2-psMan-O-CH₂CH₂NH₂ **1a**. a) Cu(OTf)₂, BrCH₂CH₂OH, 41%; b) NaN₃, DMF, 50 °C, 89%; c) **6**, TMSOTf, -20 °C, 48%; d) NaOMe, MeOH, 95%; e) H₂, Pd(c), MeOH, RT, 100%.

features a short tether terminated by either an azido (**1c**) or an amino (**1a**) group (Scheme 1). This structure is a good candidate to generate new multivalent DC-SIGN ligands that may display enhanced metabolic stability. The interaction of **1c** with the DC-SIGN extracellular (EC) domain was studied in so-

lution by NMR spectroscopy and a model of the DC-SIGN–compound **1** complex was obtained by docking studies. The antiviral activity of **1a** was tested using an infection model based on pseudotype Ebola virus and Jurkat cells expressing DC-SIGN and was found to be superior to that of its natural counterpart **2a**.

Results and Discussion

Synthesis

The synthesis of the pseudomannobiose **1a** is described in Scheme 1. Starting from the known epoxide **3**,^[9] the enantiopure scaffold **5** (Scheme 1) was synthesized by a Cu(OTf)₂-promoted epoxide opening with 2-bromoethanol to afford **4**, that was then treated with NaN₃. The pseudodisaccharide skeleton **7** was assembled in 50% yield by glycosylation of the acceptor **5** with the tetraacetylmannose trichloroacetimidate **6**^[10–12] (Scheme 1). The reaction was promoted by 0.4 mol equiv of TMSOTf in CH₂Cl₂ at -20 °C. Deacetylation (MeONa in MeOH) followed by azide reduction using hydrogen at one atmosphere and Pd on carbon as catalyst quantitatively afforded **1a**, whose structure was unequivocally characterized by ¹H and ¹³C NMR and by mass spectrometry.

NMR studies

The azide **1c** was selected for the NMR studies. Its interaction with the extracellular (EC) domain of DC-SIGN was studied by NMR spectroscopy at 600 MHz. Addition of the DC-SIGN EC domain to a 2 mM solution of **1c** in D₂O (d-Tris buffer, pD 8, 150 mM NaCl, 4 mM CaCl₂) induced broadening of the resonance signals in the ¹H NMR spectrum, indicating that binding occurs (Data not shown).

For ligands exchanging between free and bound state at a reasonably fast rate compared to the NMR time scale, the Saturation Transfer Difference (STD)^[13–15] and the transferred nuclear Overhauser enhancement (TR-NOESY)^[16–20] experiments can be used to observe the binding event. In STD experiments, irradiation of the protein is followed by transfer of magnetization to the ligand protons, which in turn causes a signal enhancement that can be best appreciated in the difference spectrum. STD experiments were carried out for **1c** in the presence of DC-SIGN (50:1 ligand:receptor ratio). Saturation build-up was studied between 0.4 and 2 seconds. The difference spectrum reported in Figure 2a (saturation time: 2 s) clearly shows resonance signals belonging to both the mannose residue and the cyclohexanediol moiety. This confirms that binding occurs and indicates that the ligand is in close contact with the protein. Proper quantification of the STD data was very difficult, because of signal overlap. The STD build-up curves are reported as Supporting Information.

The binding event was also analyzed by TR-NOESY experiments (50 ms mixing time). Cross peaks with the same sign as the diagonal were clearly observed at 288 K, confirming the interaction between DC-SIGN and the ligand (Figure 3). In the free state, the pseudomannobioside **1c** has two limit confor-

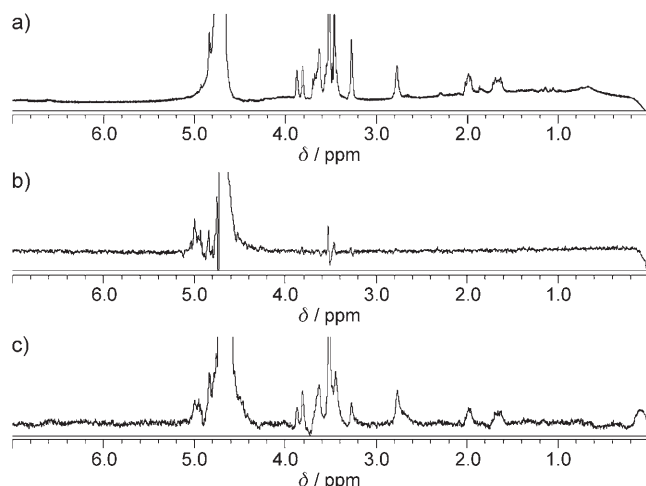


Figure 2. a) ^1H -spectrum of **1c**; b) STD experiment on **1c** as reference (1408 scans, 16 dummy scans, on-resonance frequency 0 Hz and off-resonance 12 000 Hz); c) **1c** + DC-SIGN (2.5 mM ligand and 0.05 mM protein; binding site molar ratio 50:1 in 400 μL of d-Tris, pH 8, 150 mM NaCl, 4 mM CaCl_2) STD experiment (1408 scans, 16 dummy scans, on-resonance frequency 0 Hz and off-resonance 12 000 Hz, saturation time 2 s).

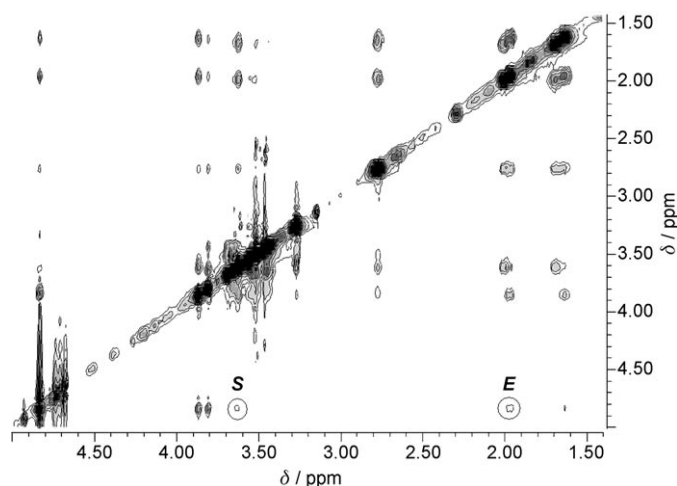


Figure 3. **1c** + DC-SIGN (2.5 mM ligand and 0.05 mM protein; binding site molar ratio 50:1 in 400 μL of d-Tris, pH 8, 150 mM NaCl, 4 mM CaCl_2) TR-NOESY experiment (mixing time 50 ms).

mations *E* and *S*, each characterized by one critical NOE cross peak.^[8] They both are present in the TR-NOESY spectrum reported in Figure 3, suggesting that both conformers may be able to interact with the protein. However, the presence of some spin diffusion noise in the spectrum does not allow definite conclusions about the preferred conformations of the ligand in the binding site to be drawn.

Docking studies

To obtain a working model for the structure of the DC-SIGN complex with **1c**, docking studies were performed starting from the PDB structure of the DC-SIGN Man4 complex (PDB code 1L4)^[21] and using the QMPolarized ligand docking protocol of Glide.^[22] In the QM-polarized ligand docking protocol, ligands are docked with Glide, then charges on the ligand induced by the protein are calculated and a set of the best ligand poses are redocked. This protocol aims to improve the partial charges on the ligand atoms by replacing them with charges derived from quantum mechanical calculations on the ligand in the field of the receptor. In this way the polarization of the charges on the ligand by the receptor is accounted for, and redocking of the ligands with these new charges can result in improved accuracy. Earlier studies performed by the Anterior group (Jianxin Duan, Jörg Weiser, personal communication) have validated this protocol for the DC-SIGN case using the available X-ray structures.^[2,21] We had previously shown that in water solution the pseudomannobiosides **1** adopt two rapidly interconverting conformations that differ in the rotation around the ψ inter(pseudo)glycosidic bond C1-O1-C2'-C1' and are equivalent to the stacked (*S*) and extended (*E*) conformations described for 1,2-mannobioside.^[8] These two were used as starting points for the docking run. The methyl ether glycoside **1b** ($\text{R} = \text{Me}$) was used as a convenient computational model of **1**.

All complexes obtained appeared to maintain the interactions between the Ca^{++} atom and two hydroxy groups of the nonreducing end mannose unit. The twenty final poses were subjected to cluster analysis using the inter(pseudo)glycosidic dihedral angles ϕ (O5-C1-O1-C2') and ψ (C1-O1-C2'-C1'). The top ranked pose (Figure 4a, Gscore = -6.40) belongs to the most populated cluster and the pseudo-mannobioside adopts a stacked conformation ($\phi = 76^\circ$ $\psi = -78^\circ$). The second cluster contains the extended conformations. The lead member features a Gscore = -6.13 and a distorted conformation with a ϕ value of 156° (Figure 4b). α -Glycosides such as **1** are subjected to a strong *exo*-anomeric effect which forces ϕ to maintain a *gauche* conformation.^[23] Therefore this value is likely to be an artifact due to the simplified conformational search procedures

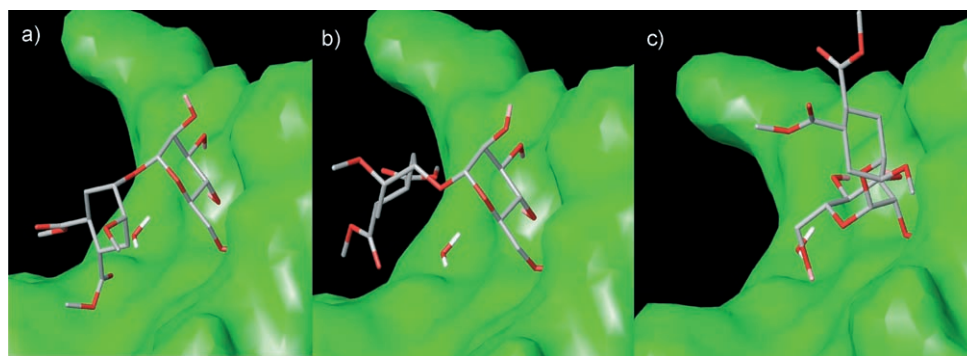


Figure 4. a) Top ranked pose from docking (QM-polarized Glide) of **1b** ($\text{R} = \text{Me}$) in DC-SIGN Gscore = -6.40 ($\text{Ph} = 76^\circ$ $\text{Psi} = -78^\circ$); b) "Extended" pose Gscore = -6.13 ($\text{Phi} = 156^\circ$ $\text{Psi} = -131^\circ$); c) The third cluster lead member G = -6.12 ($\text{Phi} = 156^\circ$ $\text{Psi} = -80^\circ$).

used by Glide during the flexible docking phase. The lead member of the third cluster (Figure 4c, Gscore = -6.12) is a stacked conformation but the dihedral ϕ is again distorted at 156°.

Infection Studies

The antiviral activity of **1a** was tested using an infection model based on Ebola envelope-pseudotyped viruses and Jurkat cells expressing DC-SIGN.^[24] These cells are permissive to this type of virus and this infection model has been used previously by our group to test the antiviral activity of multivalent carbohydrate ligands.^[25] The activity of **1a** in this infection model was compared with the natural disaccharide derivative **2a** presenting the same linker at the anomeric position. Different concentrations of compounds **1a** and **2a** were used up to a concentration of 10 mM and assays were repeated at least three times

for each concentration. The results found in this study are represented in Figure 5.

The curves represent a clear dose dependent inhibition activity for both compounds. The analysis of the curves shown in Figure 5 allows estimation of the IC₅₀ for each compound. The IC₅₀ measured for the mimic **1a** was 0.62 mM, approximately three times lower than the IC₅₀ value estimated for the corresponding disaccharide **2a** (1.91 mM). This biological model showed that the designed pseudodisaccharide **1a** is a stronger inhibitor than the corresponding disaccharide **2a** and taking into account its enzymatic stability could be considered as a promising candidate to prepare multivalent systems to be used as inhibitors of viral infection.

Conclusions

We have synthesized a pseudo-1,2-mannobioside with a short linker at the anomeric position suitable for preparation of the corresponding multivalent systems. The synthesis is very simple, and the compound can be easily prepared in gram scale. The binding process between this compound and DC-SIGN was analyzed by NMR and the information was complemented by docking studies in silico that yielded a reasonable picture of the binding mode. The results from the NMR studies so far do not allow discrimination among the models obtained computationally, nor do they allow any further refinement. At this stage we regard the structures shown in Figure 4 as a reasonable working model, which can be used to support further ligand design.

Infection studies were carried out using an Ebola infection model and proved that the glycomimetic compound **1a** inhibits infection of DC-SIGN expressing Jurkat cells more efficiently than the corresponding natural disaccharide. The inhibitory concentration of **1a** in the infection experiments was found to be in the low millimolar range, as expected for small, monovalent ligands interacting with DC-SIGN. However, the results obtained indicate that these types of mimic compounds are good candidates to prepare high affinity multivalent systems with the aim to interact and block the receptor DC-SIGN. The advantage presented by this type of ligand in terms of stability against glycosidases converts these mimic compounds in very attractive ligands for developing new antiviral drugs. Preparation of multivalent systems and evaluation of the corresponding activities are underway.

Experimental Section

Synthesis: NMR spectra were recorded at 25 and 30 °C on Bruker spectrometers. The cyclohexanediol moiety is numbered as in Figure 1. Subscripts D refer to the cyclohexanediol (ps-Man) residue of **7** and **1**. Chemical shifts ¹H and ¹³C NMR spectra are expressed in ppm relative to TMS or to DSS for spectra recorded in D₂O. Mass spectrometry was performed with a VG 7070 EQ-HF apparatus (FAB ionization), or an Omnix apparatus (MALDI ionization), or Apex II ICR FTMS (ESI ionization - HR-MS). Optical rotations [α]_D were measured in a 1-dm path-length cell with 1 mL capacity on a Perkin-Elmer 241 polarimeter. Thin layer chromatography (TLC) was carried out with precoated Merck F254 silica gel plates.

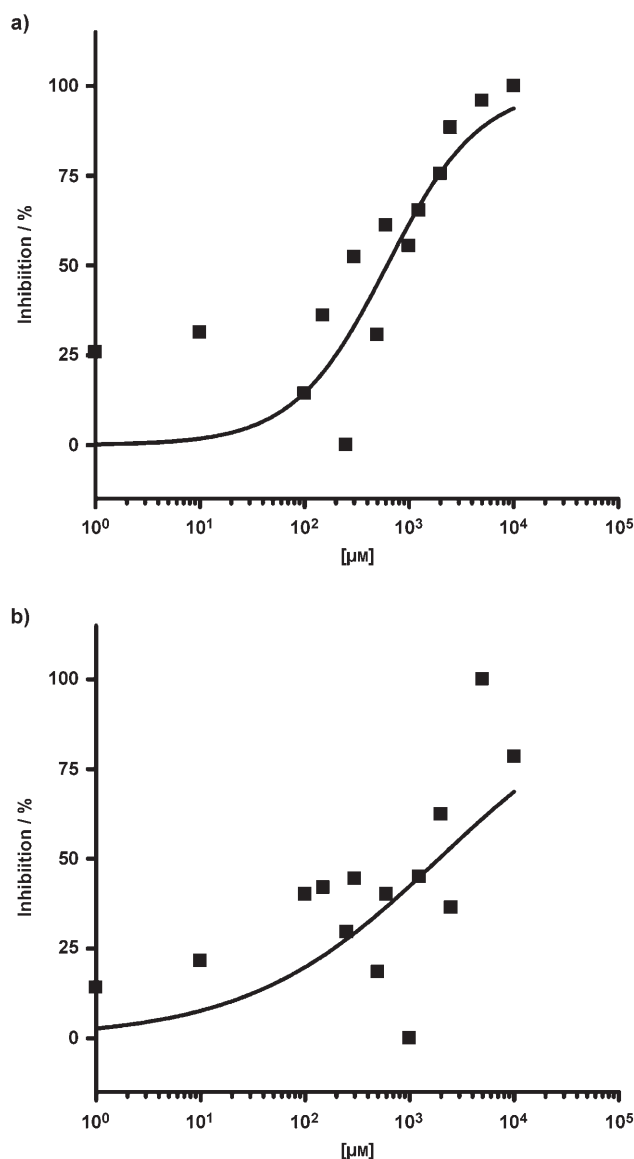


Figure 5. Inhibition of Infection results for compounds a) **1a** and b) **2a**.

Flash chromatography (FC) was carried out with Macherey–Nagel silica gel 60 (230–400 mesh). Solvents were dried by standard procedures and reactions requiring anhydrous conditions were run under nitrogen. The epoxide **3**^[9] and the trichloroacetimidate **6**^[10–12] were prepared by published procedures.

Dimethyl (1S,2S,4S,5S)-1-(2-bromoethoxy)-2-hydroxycyclohexane-4,5-dicarboxylate 4: 2-bromoethanol (600 μ L, 8.45 mmol, 4 equiv) and Cu(OTf)₂ (81 mg, 0.224 mmol, 0.11 equiv) were added to a solution of the epoxide **3**^[9] (447 mg, 2.09 mmol, 1 equiv) in dry CH₂Cl₂ (5 mL). The solution was stirred at room temperature for 3 h, following the progress by TLC (6:4 hexane:AcOEt) before quenching with 1:1 NH₄Cl_{sat} and NH₄OH and extracting with AcOEt. The organic phase was washed twice with a saturated water solution of NH₄Cl and then with water. The organic phase was dried over Na₂SO₄ and the solvent evaporated to yield a crude yellow oil (646 mg), which was purified by flash chromatography (6:4 hexane: AcOEt) to afford 281 mg of pure **4** (41 %). [α]_D²⁰ = +3.7 (*c* = 1.55 in chloroform); ¹H NMR (400 MHz, C₆D₆): δ = 1.95 (dt, *J*_{gem} = 14 Hz, *J*_{3eq,2} = *J*_{3eq,4} = 4 Hz, 1H; H_{3eq}), 2.08 (m, 2H, H₆), 2.18 (dt, *J*_{gem} = *J*_{3ax,4} = 14 Hz, *J*_{3ax,2} = 2.5 Hz, 1H; H_{3ax}), 3.00 (t, *J*_{8,7} = 4 Hz, 2H; CH₂Br), 3.15–3.25 (m, 2H; H₁, CH₂O), 3.30–3.50 (m, 9H; CH₂O, H₄, H₅, 2 OCH₃), 3.70 ppm (q, *J*_{2,3ax} = *J*_{2,3eq} = *J*_{2,1} = 2.5 Hz, 1H; H₂); ¹³C NMR (100.6 MHz, C₆D₆): δ = 27.3 (C₆); 30.7 (C₃); 30.8 (CH₂Br); 39.0 (C₅); 39.5 (C₄); 51.3 (2×OMe); 66.8 (C₂); 68.8 (CH₂O); 76.9 (C₁); 174.7 ppm (C=O); HR-MS (ESI): calculated for C₁₂H₁₉BrO₆ [M+Na]⁺: 361.02572; found [M+Na]⁺: 361.02525.

Dimethyl (1S,2S,4S,5S)-1-(2-azidoethoxy)-2-hydroxycyclohexane-4,5-dicarboxylate 5: NaN₃ (527 mg, 8.11 mmol) was added to a solution of the bromide **4** (275 mg, 0.811 mmol) in DMF (8 mL). The mixture was stirred under N₂ at 50 °C for two days. AcOEt was added; the organic phase was washed with water then dried over Na₂SO₄. The solvent was evaporated under reduced pressure, to yield 217 mg of **5** (89%), that was used for the mannosylation reaction without further purification. [α]_D²⁰ = +19.2 (*c* = 1.15 in chloroform); ¹H NMR (400 MHz, C₆D₆): δ = 1.97 (dt, *J*_{gem} = 13.6 Hz, *J*_{3eq,4} = *J*_{3eq,2} = 4.4 Hz, 1H; H_{3eq}), 2.08 (m, 2H, H₆), 2.18 (dt, *J*_{gem} = *J*_{3ax,4} = 13.6 Hz, *J*_{3ax,2} = 2.8 Hz, 1H; H_{3ax}), 2.68 (m, 1H, CH₂N₃); 2.78 (m, 1H, CH₂N₃), 3.03 (ddd, *J*_{gem} = 10.4 Hz, *J*_{7,8a} = 3.6 Hz, *J*_{7,8b} = 7.6 Hz, 1H; CH₂O), 3.20–3.28 (m, 2H, H₁; CH₂O), 3.30–3.50 (m, 2H; H₄, H₅), 3.47 (s, 3H; OCH₃), 3.48 (s, 3H; OCH₃), 3.75 ppm (bs, 1H; H₂); ¹³C NMR (100.6 MHz, C₆D₆): δ = 26.5 (C₆); 30.8 (C₃); 39.0 (C₅); 39.4 (C₄); 51.1 (OMe); 51.2 (OMe); 55.9 (CH₂N₃); 66.6 (C₂); 66.7 (CH₂O); 77.7 (C₁); 174.9 ppm (C=O); IR (KBr): $\tilde{\nu}$ = 2103; HR-MS (ESI): calculated for C₁₂H₁₉O₆N₃Na [M+Na]⁺: 324.11661; found [M+Na]⁺: 324.11624.

Synthesis of the protected pseudo-1,2-mannobioside 7: The trichloroacetimidate **6**^[10–12] (518 mg, 1.05 mmol) and the alcohol **5** (207 mg, 0.688 mmol) were dried overnight over acid-washed molecular sieves, then they were dissolved in dry CH₂Cl₂ (11 mL). TMSOTf (50 μ L, 0.275 mmol) was added under nitrogen at –20 °C and the reaction was stirred for 25 min monitoring by TLC (95:5 CH₂Cl₂: acetone). Et₃N (80 μ L) was added, the mixture was filtered through a celite pad and the solvent evaporated. The crude was purified by flash chromatography (95:5 CH₂Cl₂:acetone) to yield 200 mg of pure **7** (48 %); [α]_D²⁰ = +33.3 (*c* = 1.10 in chloroform); ¹H NMR (400 MHz, C₆D₆): δ = 1.75 (s, 3H; OCOCH₃), 1.80 (s, 3H; OCOCH₃), 1.82 (s, 3H; OCOCH₃), 1.89 (s, 3H; OCOCH₃), 2.03–2.13 (m, 4H; H_{3D}, H_{6D}), 2.74–2.87 (m, 2H; CH₂N₃), 3.13–3.20 (m, 1H; CH₂O), 3.23–3.38 (m, 3H; H_{4D}, H_{5D}, CH₂O), 3.4 (s, 3H; OCH₃), 3.46 (s, 3H; OCH₃), 3.46 (m, 1H; H_{2D}), 3.95 (m, 1H; H_{1D}), 4.35 (m, 1H; H₅), 4.40 (dd, *J*_{gem} = 12.4 Hz, *J*_{6a-5} = 2.4 Hz, 1H; H_{6a}), 4.52 (dd, *J*_{gem} = 12.4 Hz, *J*_{6b-5} = 6 Hz, 1H; H_{6b}), 5.16 (d, *J*₁₋₂ = 2 Hz, 1H; H₁), 5.65 (dd, *J*₁₋₂ = 2 Hz, *J*₂₋₃ = 3.5 Hz, 1H; H₂), 5.81 (t, *J*₃₋₄ = *J*₄₋₅ = 10 Hz, 1H; H₄), 5.88 ppm (dd, *J*₃₋₄ = 10 Hz, *J*₂₋₃ = 3.5 Hz, 1H; H₃); ¹³C NMR (100 MHz, C₆D₆): δ = 20.6, 20.65, 20.7 (CH₃C=O); 27.5 (C_{6D}); 28.5 (C_{3D}); 39.9

(C_{5D}); 40 (C_{4D}); 51.5 (CH₂N₃); 52; 63, 67.5; 69; 70; 70.5; 71; 73; 76; 96 (C₁); 170, 170.5, 175 ppm; HR-MS (ESI): calculated for C₂₆H₃₇N₃O₁₅ [M+Na]⁺: 654.21169; found [M+Na]⁺: 654.21075.

Synthesis of the pseudo-1,2-mannobioside 1c: 50 μ L of a 1 M solution of NaOMe (0.05 mmol, 0.16 equiv) in MeOH were added to a solution of the protected pseudo-1,2-mannobioside **7** (197 mg, 0.312 mmol, 1 equiv) in MeOH (3.2 mL). The reaction was stirred for 20 min monitoring by TLC (1:1 hexane : AcOEt). Amberlite IR 120 H⁺ was added until pH 7, the beads were filtered off and washed with MeOH. Solvent was evaporated under reduced pressure, to yield 137 mg of the product **1c** (95%), that was used without further purification. [α]_D²⁰ = +80.0 (*c* = 0.65 in methanol); ¹H NMR (600 MHz, D₂O, pD 8 Tris-d buffer): δ = 1.64 (app t, *J* = 12 Hz, 1H; H_{3Dax}), 1.69 (app t, *J* = 12 Hz, 1H; H_{6Dax}), 1.96–2.02 (m, 2H; H_{3Deq}, H_{6Deq}), 2.79 (m, 2H; H_{4D}, H_{5D}), 3.28 (m, 2H; CH₂N₃), 3.45 (m, 1H; H₄), 3.46 (m, 4H; OCH₃, H₅), 3.52 (m, 4H; OCH₃, H_{6a}), 3.56 (m, 1H; H_{6b}), 3.82 (bs, 1H; H₂), 3.88 (bs, 1H; H_{2D}), 4.85 ppm (bs, 1H; H₁); ¹³C NMR (150 MHz, D₂O): δ = 26.5 (C_{3D}), 27 (C_{6D}), 39 (C_{4D} and C_{5D}), 50.5 (CH₂N₃), 53 (COOMe), 60 (COOMe), 61 (C₆), 66.5 (C₄), 67.5 (CH₂O), 70 (C₂, C₃), 70.5 (C_{2D}), 73 (C₅), 74 (C_{1D}), 98.5 ppm (C₁); HR-MS (ESI): calculated for C₁₈H₂₉N₃O₁₁ [M+Na]⁺: 486.16943; found [M+Na]⁺: 486.16870.

Synthesis of the pseudo-1,2-mannobioside 1a: Azide **1c** (130 mg, 0.28 mmol) was dissolved in MeOH (10 mL), and Pd-C 10% (cat.) was added. The reaction mixture was hydrogenated (1 bar) at room temperature until reduction was complete monitoring by TLC (CH₂Cl₂-MeOH, 7:3) to afford 122 mg of amine **1a** (100%) as a white solid. [α]_D²⁰ = +48.3 (*c* = 0.60 in methanol); ¹H NMR (500 MHz, D₂O): δ = 1.68 (m, 1H; H_{6Dax}), 1.71 (m, 1H; H_{3Deq}), 1.98 (m, 1H; H_{3Deq}), 2.06 (m, 1H; H_{6Dax}), 2.85 (m, 2H; H_{4D} and H_{5D}), 2.96 (m, 2H; CH₂NH₂), 3.50–3.70 (m, 6H; H₄, H₅, H_{6A}, H_{1D}, CH₂O), 3.60 (s, 6H; 2×COOMe), 3.70–3.80 (m, 2H; H_{6B} and H₃), 3.89 (dd, *J* = 1.5 and 3.0 Hz, 1H; H₂), 3.93 (m, 1H; H_{2D}), 4.93 (bs, 1H; H₁); ¹³C NMR (125 MHz, D₂O): δ = 26.5 (C_{3D}), 26.9 (C_{6D}), 38.9 and 39.7 (C_{4D} and C_{5D}), 42.0 (CH₂NH₂), 52.3 (COOMe), 52.6 (COOMe), 61.0 (C₆), 66.8 (CH_{2O}), 70.4 (C₂ and C₃), 70.8 (C_{2D}), 74.3 (C₅), 75.0 (C_{1D}), 98.5 (C₁), 178.5 (CO), 178.6 (CO); HR-MS (ESI): calculate for C₁₈H₃₁NO₁₁ [M+Na]⁺: 460.17893; found [M+Na]⁺: 461.17826.

NMR studies: The spectra were recorded at 288 K on a 600 MHz using a 2 mm solution of **1c** in D₂O (d-Tris buffer, pD 8, 150 mM NaCl, 4 mM CaCl₂) and a 50:1 molar ratio of **1c** and the EC domain of DC-SIGN. STD experiments were carried out at two frequencies 0 and 300 Hz (corresponding to 0 and 0.5 ppm), where ligand signals were not affected. For all the irradiating resonances, five STD experiments were carried out with an increasing saturation time of protein resonances: 400 ms, 800 ms, 1.2 s, 1.6 s and 2 s. TR-NOESY experiments were also performed on the same solution using 50 ms of mixing time and suppressing the water signal.

Computational methods: All calculations were run using the Schrodinger suite of programs (<http://www.schrodinger.com>) through the Maestro graphical interface.

Protein Setup: In the protein data bank three high-resolution X-ray crystal structures of human DC-SIGN complex with oligosaccharides are stored with the following PDB entry codes: 1L4.pdb, 1L5.pdb, and 1K9I.pdb. The binding determinant of the ligand in 1K9I and in 1L4 is a mannose unit, in 1L5 it is a fucose residue belonging to the Lewis-x (Fuc α 1,3-(Gal β 1,4)-GlcNAc) fragment of LNFP. Both monosaccharides interact with the Ca⁺⁺ atom, but the remaining part of the binding region is quite different for the two ligands. Starting from the coordinates taken from the structure with 1L4 pdb code (crystal structure of the DC-SIGN carbohydrate recognition domain complexed with Man₄) a molecular model of the protein to use in docking studies was prepared. This X-ray crys-

tal structure was chosen because it has the best resolution of the group deposited so far. The protein was set up as follows: all water molecules were removed except one (PDB code HOH 19) that is conserved in 1L4, 1L5, and 1K9I and bridges between the ligands and the protein. Charged groups neither located in the ligand-binding pocket nor in salt bridges were neutralized using Schrödinger pprep script (First Discovery 2.5 User Manual). Hydrogens were added using Maestro, side chains and hydrogens added were optimized using Schrödinger impref script (First Discovery 2.5 User Manual), (RMSD between X-ray structure and output of impref was 0.372 Å).

As described above, the binding region of DC-SIGN is potentially quite extended, and this feature should be taken into account when building a docking model. This was done by defining a "superligand" taken from 1L4 (mannose-based ligand) and 1L5 (fucose-based ligand), and defining the active shell of protein residues for the molecular calculations starting from this virtual structure. The reference ligand (Man4) was subjected to a minimization in the ligand binding pocket using a substructure built as follows: the atoms within 10 Å from the superligand were unconstrained during the calculations; the force constants used for the restraining potentials were distance dependent relative to the superligand with the following parabolic force constants for the constrained atoms: 10–15 Å $k = 50 \text{ kJ Å}^{-1}$; 15–20 Å $k = 100 \text{ kJ Å}^{-1}$; 20–25 Å $k = 200 \text{ kJ Å}^{-1}$; the Ca^{++} atoms and oxygen atom of water were constrained with $k = 100 \text{ kJ Å}^{-1}$; the part of the protein outside these shells were frozen. The Macromodel/batchmin software package (version 8.5) employing the AMBER* force field was used for minimization.^[26,27] Bulk water solvation was simulated using Macromodel's generalized Born GB/SA continuum solvent model.^[28] Energy minimization was performed using truncated Newton conjugate gradient (TNCG) procedure and was terminated either after 500 iterations or when the energy gradient RMS fell below 0.05 kJ Å^{-1} . This minimized structure was employed as receptor structure in the grid generation and as reference structure in the docking studies.

Docking: Starting from the minimized complex described above, structural models for the interaction of the pseudomannobioside with the ligand binding site of the DC-SIGN receptor were generated by automated computational docking using the QMPolarized ligand docking protocol of Glide^[22] after removal of the oligosaccharide ligand. In the QM-polarized ligand docking protocol, ligands are docked with Glide, then charges on the ligand induced by the protein are calculated with Qsite, and a set of the best ligand poses are redocked.

Glide (Grid-based Ligand Docking with Energetics) calculations were performed with Impact^[29] version 4.0 and Qsite calculations were performed with Jaguar version 6.5 (L. Schrödinger). Glide uses a hierarchical series of filters to search for possible locations of the ligand in the active-site region of the receptor. The shape and properties of the receptor are represented on a grid by several different sets of fields that provide progressively more accurate scoring of the ligand poses. To begin the Glide calculation an enclosing box and a bounding box are defined starting from the center of the reference ligand. The starting poses for the ligands to be screened are generated by placing the center of the ligand in random points of the bounding box. Conformational flexibility is handled in Glide by an extensive conformational search, augmented by a heuristic screen that rapidly eliminates conformations deemed unsuitable for binding to a receptor, such as conformations that have long-range internal hydrogen bonds. After all the filters have been applied, the remaining best 400 poses are partially minimized in the grid field using the OPLSAA force field and finally scored using the GlideScore scoring function. GlideScore is

based on ChemScore,^[30] but includes a steric clash term and adds buried polar terms to penalize electrostatic mismatches.

The grid generation step started from the minimized structure of the DC-SIGN: Man₄ complex (from 1L4) described in the protein setup section and used mae input files of both ligand and active site, including hydrogen atoms. The center of the grid enclosing box was defined by the center of the bound Man₄ ligand. The enclosing box dimensions, which are automatically deduced from the ligand size, fit the entire active site. For the docking step, the size of bounding box for placing the ligand center was set to 10 Å.

In the receptor grid generation the metal constraint was employed. No further modifications were applied to the default settings. The protocol carried out for the QM polarized ligand docking was the following: initial docking: SP, poses saved: 5, Qsite setting: fast, final docking: SP. The GlideScore function was used to select ten poses for each ligand.

With this computational protocol automated docking calculations starting from the two representative conformations of pseudomannobioside, stacked and extended,^[8] were performed. The methyl ether derivative **1b** ($R = \text{Me}$) was used as a computationally convenient model.

The 20 higher ranking poses were subjected to cluster analysis using Xcluster (Macromodel 9.1—Xcluster manual) and the interglycosidic angles ϕ (O5-C1-O1-C2') and ψ (C1-O1-C2'-C1') were used as variables

DC-SIGN EC expression and purification: Plasmids pET30b (Novagen) containing cDNA encoding the EctoDomain ECD (corresponding to amino acids 66–404) of DC-SIGN were used for overproduction as described previously.^[31] Proteins produced in inclusion bodies have been refolded as already described.^[3] Purification of functional DC-SIGN proteins were achieved by an affinity chromatography on mannan-agarose column (Sigma) equilibrated in 25 mM Tris-HCl pH 7.8, 150 mM NaCl, 4 mM CaCl_2 (Buffer A), and eluted in the same buffer lacking CaCl_2 but supplemented with 10 mM EDTA. This step was followed by a superose 6 size exclusion chromatography equilibrated in buffer A. Protein was concentrated to 9 mg mL^{-1} and dialyzed three times against the deuterated buffer 25 mM Tris DCl, 150 mM NaCl, 4 mM CaCl_2 at pD 7.8 in D_2O (deuterated Tris-d11 (98%) was purchased from Cambridge Laboratories Inc. and the D_2O from Spectra Stable Isotopes). Protein was then stored in liquid nitrogen.

Cell culture and Reagents: 293FT cells obtained from Invitrogen were grown in Dulbecco's Modified Eagle Medium (D-MEM, Cambrex, Verviers, Belgium) supplemented with 10% heat-inactivated Fetal Bovine Serum, 2 mM L-glutamine, and $50 \mu\text{g mL}^{-1}$ gentamicin. Jurkat cells stably expressing DC-SIGN^[24] were grown in RPMI 1640 medium (Cambrex) supplemented with 10% Fetal Bovine Serum, 2 mM L-glutamine (Sigma) and $50 \mu\text{g mL}^{-1}$ gentamicin.

Pseudovirus production: The lentiviral vector pNL4-3.Luc.R-E (obtained from Nathaniel Landau through the AIDS Research and Reference Reagent Program, Division of AIDS, National Institute of Allergy and Infectious Disease, National Institute of Health, Rockville, Maryland) was used for the production of vesicular stomatitis virus G protein (VSVG) and EboZV GP-pseudotyped lentivirus. Expression plasmid for the GP of the Zaire Ebola virus was kindly provided by A. Sánchez, Centers for Disease Control and Prevention, Atlanta, Ga. These viruses were produced according to a transient-transfection protocol using 293FT cells. Briefly, virus producer cells (293FT) were seeded at 6.0×10^6 cells in 100 mm plates 1 day before transfection. Cells were cotransfected using a calcium phosphate transfection kit (Invitrogen). Supernatants were harvested after 48 h, centrifuged at $300 \text{ g } 10'$ at RT to remove cell debris, and stored frozen at -80°C .

Infection Assay: To determine the role of compounds **1a** and **2a** in inhibiting the infection of EboZV GP-pseudotyped lentivirus, 200,000 Jurkat DC-SIGN cells were preincubated with serial dilutions of compounds for 30' at 37 °C and 5% CO₂. Cells were infected with Ebola GP-pseudotyped lentivirus at a MOI of 0.1 and VSVG-pseudotyped lentiviruses as control, to rule out nonspecific neutralization. Cells were lysed 48 h after infection, and the lysate was evaluated with a luciferase assay (reagents from Promega, Madison, WI, USA), in a Berthold Sirius luminometer (Berthold, Munich, Germany) with a dynamic range of 10²–10⁷ relative luminescence units (RLUs). Statistics: Fifty percent inhibitory concentrations (IC₅₀) were calculated in GraphPad Prism 4.

Acknowledgements

We want to acknowledge financial support from the FIS to J. R. (PI030093) and R. D. (PI030300) and Ensemble contre le SIDA, Sidaaction to F. F. This research has been supported in part by the European Community in the form of a Marie Curie Fellowship (to J.J.R.) of the programme IHP under contract number HPMT-CT-2001-00293.

Keywords: antiviral activity • carbohydrate mimics • DC-SIGN • docking • mannose

- [1] T. B. H. Geijtenbeek, R. Torensma, S. J. Van Vliet, G. C. F. van Duijnhoven, G. J. Adema, Y. van Kooyk, C. G. Figdor, *Cell* **2000**, *100*, 575–585.
- [2] H. Feinberg, D. A. Mitchell, K. Drickamer, W. I. Weis, *Science* **2001**, *294*, 2163–2166.
- [3] D. A. Mitchell, A. J. Fadden, K. Drickamer, *J. Biol. Chem.* **2001**, *276*, 28939–28945.
- [4] Y. van Kooyk, T. B. H. Geijtenbeek, *Nat. Rev. Immunol.* **2003**, *3*, 697–709.
- [5] D. A. Calarese, C. N. Scanlan, M. B. Zwick, S. Deechongkit, Y. Minura, R. Kunert, P. Zhu, M. R. Wormald, R. L. Stanfield, K. H. Roux, J. W. Kelly, P. M. Rudd, R. A. Dwek, H. Kattinger, D. R. Burton, I. A. Wilson, *Science* **2003**, *300*, 2065–2071.
- [6] D. A. Calarese, H.-K. Lee, C.-Y. Huang, M. D. Best, R. D. Astronomo, R. L. Stanfield, H. Kattinger, D. R. Burton, C. H. Wong, I. A. Wilson, *Proc. Natl. Acad. Sci. USA* **2005**, *102*, 13372–13377.
- [7] E. W. Adams, D. M. Ratner, H. R. Bokesch, J. B. McMahon, B. R. O'Keefe, P. H. Seeberger, *Chem. Biol.* **2004**, *11*, 875–881.
- [8] S. Mari, H. Posterl, G. Marcou, D. Potenza, F. Micheli, F. J. Canada, J. Jimenez-Barbero, A. Bernardi, *Eur. J. Org. Chem.* **2004**, 5119–5225.
- [9] A. Bernardi, D. Arosio, L. Manzoni, F. Micheli, A. Pasquarello, P. Seneci, *J. Org. Chem.* **2001**, *66*, 6209–6216.
- [10] T. Ren, D. Liu, *Tetrahedron Lett.* **1999**, *40*, 7621–7625.
- [11] R. R. Schmidt, J. Michel, *Angew. Chem.* **1980**, *92*, 763–764; *Angew. Chem. Int. Ed. Engl.* **1980**, *19*, 731–732.
- [12] R. R. Schmidt, *Angew. Chem.* **1986**, *98*, 213–236; *Angew. Chem. Int. Ed. Engl.* **1986**, *25*, 212–235.
- [13] M. Mayer, B. Meyer, *Angew. Chem.* **1999**, *111*, 1902–1906; *Angew. Chem. Int. Ed.* **1999**, *38*, 1784–1788.
- [14] J. Klein, R. Meinecke, M. Meyer, B. Meyer, *J. Am. Chem. Soc.* **1999**, *121*, 5336–5337.
- [15] M. Vogtherr, T. Peters, *J. Am. Chem. Soc.* **2000**, *122*, 6093–6099.
- [16] A. A. Bothner-By, R. Gassend, *Ann. N. Y. Acad. Sci.* **1973**, *222*, 668–676.
- [17] P. L. Jackson, H. N. Moseley, N. R. Krishna, *J. Magn. Reson. Ser. B* **1995**, *107*, 289–292.
- [18] V. L. Bevilacqua, D. S. Thomson, J. H. Prestegard, *Biochemistry* **1990**, *29*, 5529–5537.
- [19] V. L. Bevilacqua, Y. Kim, J. H. Prestegard, *Biochemistry* **1992**, *31*, 9339–9349.
- [20] H. Kogelberg, D. Solís, J. Jiménez-Barbero, *Curr. Opin. Struct. Biol.* **2003**, *13*, 646–653.
- [21] Y. Guo, H. Feinberg, E. Conroy, D. A. Mitchell, R. Alvarez, O. Blixt, M. E. Taylor, W. I. Weis, K. Drickamer, *Nat. Struct. Mol. Biol.* **2004**, *11*, 591–598.
- [22] A. E. Cho, V. Guallar, B. J. Berne, R. Friesner, *J. Comput. Chem.* **2005**, *26*, 915–931.
- [23] V. S. R. Rao, P. K. Qasba, P. V. Balaji, R. Chandrasekaran *Conformation of carbohydrates*, Harwood Academic Publishers, Amsterdam, **1998**.
- [24] C. P. Alvarez, F. Lasala, J. Carrillo, O. Muñiz, A. L. Corbí, R. Delgado, *J. Virol.* **2002**, *76*, 6841–6844.
- [25] F. Lasala, E. Arce, J. R. Otero, J. Rojo, R. Delgado, *Antimicrob. Agents Chemother.* **2003**, *47*, 3970–3972.
- [26] S. J. Weiner, P. A. Kollman, D. A. Case, U. C. Singh, C. Ghio, G. Alagona, S. Profeta, P. Weiner, *J. Am. Chem. Soc.* **1984**, *106*, 765–784.
- [27] S. J. Weiner, P. A. Kollman, D. T. Nguyen, D. A. Case, *J. Comput. Chem.* **1986**, *7*, 230–252.
- [28] W. C. Still, A. Tempczyk, R. C. Hawley, T. Hendrickson, *J. Am. Chem. Soc.* **1990**, *112*, 6127–6129.
- [29] J. L. Banks, H. S. Beard, Y. Cao, A. E. Cho, W. Damm, R. Farid, A. K. Felts, T. A. Halgren, D. T. Mainz, J. R. Maple, R. Murphy, D. M. Philipp, M. P. Repasky, L. Y. Zhang, B. J. Berne, R. A. Friesner, E. Gallicchio, R. M. Levy, *J. Comput. Chem.* **2005**, *26*, 1752–1780.
- [30] M. D. Eldridge, C. W. Murray, T. R. Auton, G. V. Paolini, R. P. Mee, *J. Comput.-Aided Mol. Des.* **1997**, *11*, 425–445.
- [31] F. Halary, A. Amara, H. Lortat-Jacob, M. Messerle, T. Delaunay, C. Houlès, F. Fieschi, F. Arenzana-Seisdedos, J.-F. Moreau, J. Déchanet-Merville, *Immunity* **2002**, *17*, 653–664.

Received: March 7, 2007

Revised: April 23, 2007

Published online on May 16, 2007